

Articles

Dioxygen-Binding Kinetics and Thermodynamics of a Series of Dicopper(I) Complexes with Bis[2-(2-pyridyl)ethyl]amine Tridendate Chelators Forming Side-On Peroxo-Bridged Dicopper(II) Adducts

Hong-Chang Liang,[†] Kenneth D. Karlin,^{*,†} Raylene Dyson,[‡] Susan Kaderli,[‡] Bernhard Jung,[‡] and Andreas D. Zuberbühler^{*,‡}

Department of Chemistry, The Johns Hopkins University, Charles & 34th Streets, Baltimore, Maryland 21218, and Institut für Anorganische Chemie, University of Basel, CH-4056 Basel, Switzerland

Received July 17, 2000

Copper–dioxygen interactions are of interest due to their importance in biological systems as reversible O₂-carriers, oxygenases, or oxidases and also because of their role in industrial and laboratory oxidation processes. Here we report on the kinetics (stopped-flow, –90 to 10 °C) of O₂-binding to a series of dicopper(I) complexes, [Cu₂(Nn)(MeCN)₂]²⁺ (**1**^{Nn}) (–(CH₂)_n– (n = 3–5) linked bis[2-(2-pyridyl)ethyl]amine, PY2) and their close mononuclear analogue, [(MePY2)Cu(MeCN)]⁺ (**3**), which form μ-η²:η²-peroxodicopper(II) complexes [Cu₂(Nn)(O₂)]²⁺ (**2**^{Nn}) and [(MePY2)Cu]₂(O₂)²⁺ (**4**), respectively. The overall kinetic mechanism involves initial reversible (*k*_{+,open}/*k*_{–,open}) formation of a nondetectable intermediate O₂-adduct [Cu₂(Nn)(O₂)]²⁺ (open), suggested to be a Cu^I...Cu^{II}–O₂[–] species, followed by its reversible closure (*k*_{+,closed}/*k*_{–,closed}) to form **2**^{Nn}. At higher temperatures (253 to 283 K), the first equilibrium lies far to the left and the observed rate law involves a simple reversible binding equilibrium process (*k*_{on,high} = (*k*_{+,open}/*k*_{–,open})(*k*_{+,closed})). From 213 to 233 K, the slow step in the oxygenation is the first reaction (*k*_{on,low} = *k*_{+,open}), and first-order behavior (in **1**^{Nn} and O₂) is observed. For either temperature regime, the Δ*H*[‡] for formation of **2**^{Nn} are low (Δ*H*[‡] = –11 to 10 kJ/mol; *k*_{on,low} = 1.1 × 10³ to 4.1 × 10³ M^{–1} s^{–1}, *k*_{on,high} = 2.2 × 10³ to 2.8 × 10⁴ M^{–1} s^{–1}), reflecting the likely occurrence of preequilibria. The Δ*H*^o ranges between –81 and –84 kJ mol^{–1} for the formation of **2**^{Nn}, and the corresponding equilibrium constant (*K*₁) increases (3 × 10⁸ to 5 × 10¹⁰ M^{–1}; 183 K) going from n = 3 to 5. Below 213 K, the half-life for formation of **2**^{Nn} increases with, rather than being independent of, the concentration of **1**^{Nn}, probably due to the oligomerization of **1**^{Nn} at these temperatures. The O₂ reaction chemistry of **3** in CH₂Cl₂ is complicated, including the presence of induction periods, and could not be fully analyzed. However, qualitative comparisons show the expected slower *intermolecular* reaction of **3** with O₂ compared to the *intramolecular* first-order reactions of **1**^{Nn}. Due to the likelihood of the partial dimerization of **3** in solution, the *t*_{1/2} for the formation of **4** remains constant with increasing complex concentration rather than decreasing. Acetonitrile significantly influences the kinetics of the O₂ reactions with **1**^{Nn} and **3**. For **1**^{N4}, the presence of MeCN inhibits the formation of a previously (Jung et al, *J. Am. Chem. Soc.* **1996**, *118*, 3763–3764) observed intermediate. Small amounts of added MeCN considerably slow the oxygenation rates of **3**, inhibit its full formation to **4**, and increase the length of the induction period. The results for **1**^{Nn} and their mononuclear analogue **3** are presented, and they are compared with each other as well as with other dinucleating dicopper(I) systems.

Introduction

Copper–dioxygen reactivity studies are of considerable interest because of their occurrence in copper-mediated oxidation,^{1–4} including O₂ processing by copper proteins.^{4–7}

These include blood dioxygen carrying hemocyanins (in arthropods and mollusks),^{6,8} oxygenases which insert O-atoms into substrates,^{5,6} and oxidases which couple substrate oxidations to copper-mediated O₂-reduction to water or H₂O₂.^{6,7,9} Thus, we have spent considerable efforts to systematically study the interaction of dioxygen with discrete copper(I) complexes, endeavoring to characterize the course of reaction, the spectroscopic features and structure of copper–dioxygen adducts, and

[†] The Johns Hopkins University.

[‡] University of Basel.

- (1) Gampp, H.; Zuberbühler, A. D. *Metal. Ions. Biol. Syst.* **1981**, *12*, 133–189.
- (2) Karlin, K. D.; Gultneh, Y. *Prog. Inorg. Chem.* **1987**, *35*, 219–327.
- (3) Kitajima, N.; Moro-oka, Y. *Chem. Rev.* **1994**, *94*, 737–757.
- (4) Karlin, K. D.; Zuberbühler, A. D. In *Bioinorganic Catalysis: Second Edition, Revised and Expanded*; Reedijk, J., Bouwman, E., Eds.; Marcel Dekker: New York, 1999; pp 469–534.
- (5) Liang, H.-C.; Dahan, M.; Karlin, K. D. *Curr. Opin. Chem. Biol.* **1999**, *3*, 168–175.

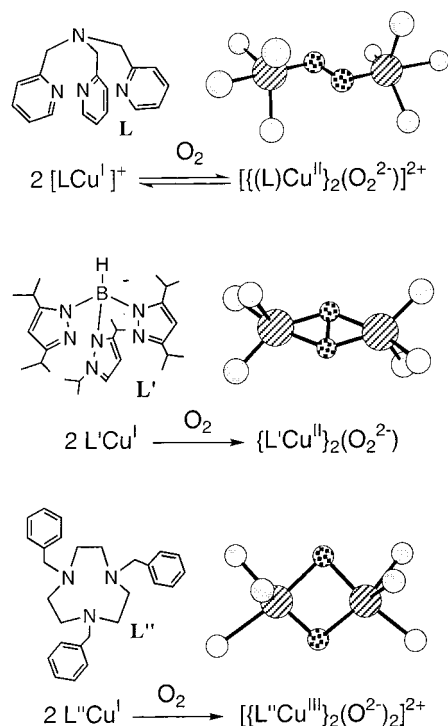
(6) Solomon, E. I.; Sundaram, U. M.; Machonkin, T. E. *Chem. Rev.* **1996**, *96*, 2563–2605.

(7) Klinman, J. P. *Chem. Rev.* **1996**, *96*, 2541–2561.

(8) Cuff, M. E.; Miller, K. I.; van Holde, K. E.; Hendrickson, W. A. *J. Mol. Biol.* **1998**, *278*, 855–870.

(9) McGuirl, M. A.; Dooley, D. M. *Curr. Opin. Chem. Biol.* **1999**, *3*, 138–144.

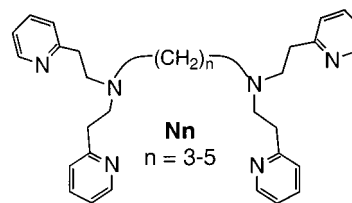
Chart 1



the subsequent reactivity of these $\{Cu_n-O_2$ (usually n is 1 or 2)} species.^{4,10,11} In this report, we provide a kinetic-thermodynamic investigation of an interesting series of Cu_2-O_2 adducts.

Several modes of O_2 -binding to copper ion complexes have been elucidated;^{4,12–14} for $Cu/O_2 = 2:1$, these include μ -1,2- (end-on) or μ - η^2 - η^2 - (side-on) peroxo-dicopper(II) coordination (Chart 1). The end-on binding mode was originally established in an X-ray structure of $[\{ (tmapa)Cu \}_2 (O_2)]^{2+}$ ($tmapa = \text{tris}(2\text{-pyridylmethyl})\text{amine}$) (Chart 1).^{15,16} However, when employing a variety of types of tridentate ligands for copper (i.e., pyridylalkylamines,^{4,17,18} trispyrazolylborates,^{3,19,20} trisimidazole phosphines,^{21,22} and triazacyclononanes²³), μ - η^2 - η^2 -peroxo-dicopper(II) binuclear species form, this being the structural type found in oxyhemocyanin and oxytyrosinase (monooxygenase).⁶

Chart 2



With Nn type ligands (Chart 2), we first¹⁷ observed reversibly formed dioxygen adducts, $[Cu_2(Nn)(O_2)]^{2+}$, stable at $-80^\circ C$ in solution, which possess intense charge-transfer absorptions at ~ 360 nm, shown to be characteristic of this side-on peroxo coordination.²⁴ Kitajima and co-workers for the first time structurally characterized such an adduct, $[Cu(HB(3,5-iPr_2-pz)_3)_2(O_2)]$ ($3,5-iPr_2pz = \text{hydrotris}\{3,5\text{-diisopropylpyrazolyl}\}\text{-borate}$) (Chart 1).¹⁹ More recently, it has been demonstrated that trisubstituted-triazacyclononane ($iPr_3\text{-tacn}$)²⁵ (or bidentate substituted ethylenediamine,²⁶ or tetradentate 6-methyl-substituted $tmapa$)²⁷ ligand complexes of copper(I) react with O_2 affording still another type of copper(I) oxygenation product, $O-O$ cleaved bis- μ -oxo-dicopper(III) complexes (Chart 1).

The structure types observed, Chart 1, are spectroscopically distinct, and also exhibit varying reactivity patterns. In fact, even within a range of mononuclear or binuclear complexes which employ the bis[2-(2-pyridyl)ethyl]amine (PY2) moiety studied by us, many variations occur. For $[Cu_2(Nn)(O_2)]^{2+}$ O_2 -adducts 2^{Nn} , we have recently detailed the differences in UV-vis features and $O-O$ stretching vibrations (by resonance Raman spectroscopy) for the series with $N3$, $N4$, and $N5$ ligands.²⁸ The studies confirm that these molecules possess side-on μ - η^2 - η^2 -peroxo-dicopper(II) ligation, and the spectroscopic differences are ascribed to distortions of the Cu_2-O_2 moiety from planarity, probably due to binucleating ligand constraints, as depicted in Figure 1. The copper(I)/ O_2 chemistry of $[(MePY2)Cu(MeCN)]^+$ (**3**), with ligand bis[2-(2-pyridyl)ethyl]methylamine (MePY2), a mononucleating analogue of the Nn ligands, further demonstrates how a ligand can influence the resulting chemistry.²⁹ The O_2 -adduct, $[\{ (MePY2)Cu \}_2 (O_2)]^{2+}$ (**4**) exhibits a $\nu(O-O)$ value lower than any of the Nn complexes (Figure 1),^{29–31} while spectroscopically being most similar to $N5$, suggesting the Cu_2-O_2 core in **4** is planar.^{28,32} Related to Nn and MePY2 are the series of R-XYL-H ligands possessing xylyl-linked PY2 moi-

(10) Karlin, K. D.; Kaderli, S.; Zuberbühler, A. D. *Acc. Chem. Res.* **1997**, *30*, 139–147.

(11) Schindler, S. *Eur. J. Inorg. Chem.* **2000**, 2311–2326.

(12) Kopf, M.-A.; Karlin, K. D. In *Biomimetic Oxidations*; Meunier, B., Ed.; Imperial College Press: London, 2000; Chapter 7, pp 309–362.

(13) Mahadevan, V.; Klein Gebbink, R. J. M.; Stack, T. D. P. *Curr. Opin. Chem. Biol.* **2000**, *4*, 228–234.

(14) Blackman, A. G.; Tolman, W. B. In *Structure & Bonding*; B. Meunier, Ed.; Springer-Verlag: Berlin, 2000; Vol. 97, pp 179–211.

(15) Jacobson, R. R.; Tyeklar, Z.; Karlin, K. D.; Liu, S.; Zubieta, J. *J. Am. Chem. Soc.* **1988**, *110*, 3690–3692.

(16) Tyeklar, Z.; Jacobson, R. R.; Wei, N.; Murthy, N. N.; Zubieta, J.; Karlin, K. D. *J. Am. Chem. Soc.* **1993**, *115*, 2677–2689.

(17) Karlin, K. D.; Haka, M. S.; Cruse, R. W.; Gultneh, Y. *J. Am. Chem. Soc.* **1985**, *107*, 5828–5829.

(18) Kodera, M.; Katayama, K.; Tachi, Y.; Kano, K.; Hirota, S.; Fujinami, S.; Suzuki, M. *J. Am. Chem. Soc.* **1999**, *121*, 11006–11007.

(19) Kitajima, N.; Fujisawa, K.; Fujimoto, C.; Moro-oka, Y.; Hashimoto, S.; Kitagawa, T.; Toriumi, K.; Tatsumi, K.; Nakamura, A. *J. Am. Chem. Soc.* **1992**, *114*, 1277–1291.

(20) Hu, Z.; Williams, R. D.; Tran, D.; Spiro, T. G.; Gorun, S. M. *J. Am. Chem. Soc.* **2000**, *122*, 3556–3557.

(21) Lynch, W. E.; Kurtz, D. M., Jr.; Wang, S.; Scott, R. A. *J. Am. Chem. Soc.* **1994**, *116*, 11030–11038.

(22) Sorrell, T. N.; Allen, W. E.; White, P. S. *Inorg. Chem.* **1995**, *34*, 952–960.

(23) Mahapatra, S.; Halfen, J. A.; Wilkinson, E. C.; Que, L., Jr.; Tolman, W. B. *J. Am. Chem. Soc.* **1994**, *116*, 9785–9786.

(24) Baldwin, M. J.; Root, D. E.; Pate, J. E.; Fujisawa, K.; Kitajima, N.; Solomon, E. I. *J. Am. Chem. Soc.* **1992**, *114*, 10421–10431.

(25) Tolman, W. B. *Acc. Chem. Res.* **1997**, *30*, 227–237.

(26) Mahadevan, V.; Hou, Z.; Cole, A. P.; Root, D. E.; Lal, T. K.; Solomon, E. I.; Stack, T. D. P. *J. Am. Chem. Soc.* **1997**, *119*, 11996–11997.

(27) Hayashi, H.; Fujinami, S.; Nagatomo, S.; Ogo, S.; Suzuki, M.; Uehara, A.; Watanabe, Y.; Kitagawa, T. *J. Am. Chem. Soc.* **2000**, *122*, 2124–2125.

(28) Pidcock, E.; Obias, H. V.; Abe, M.; Liang, H.-C.; Karlin, K. D.; Solomon, E. I. *J. Am. Chem. Soc.* **1999**, *121*, 1299–1308.

(29) Obias, H. V.; Lin, Y.; Murthy, N. N.; Pidcock, E.; Solomon, E. I.; Ralle, M.; Blackburn, N. J.; Neuhold, Y.-M.; Zuberbühler, A. D.; Karlin, K. D. *J. Am. Chem. Soc.* **1998**, *120*, 12960–12961.

(30) In addition, solution resonance Raman spectroscopy reveals that a small percentage (<10%) of the complex exists in a bis- μ -oxo-dicopper(III) structure, showing how MePY2 confers a somewhat different chemistry than the Nn ligand complexes. Solid polycrystalline $[\{ (MePY2)Cu \}_2 (O_2)]^{2+}$ (**4**) is in fact a mixture of bis- μ -oxo-dicopper(III) and side-on peroxo-dicopper(II) species (see ref 32).

(31) $[\{ (MePY2)Cu \}_2 (O_2)]^{2+}$ (**4**) is capable of exogenous substrate hydrogen atom abstraction reactions (see ref 29).

(32) Pidcock, E.; DeBeer, S.; Obias, H. V.; Hedman, B.; Hodgson, K. O.; Karlin, K. D.; Solomon, E. I. *J. Am. Chem. Soc.* **1999**, *121*, 1870–1878.

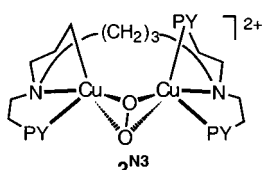
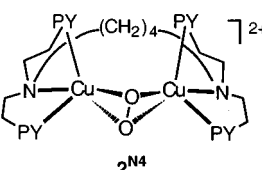
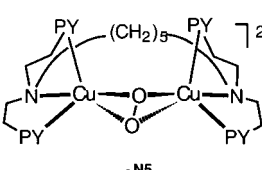
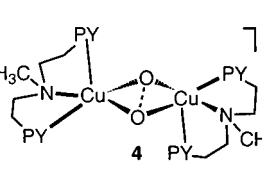
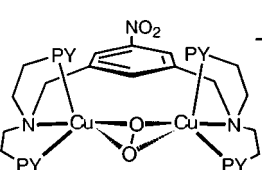
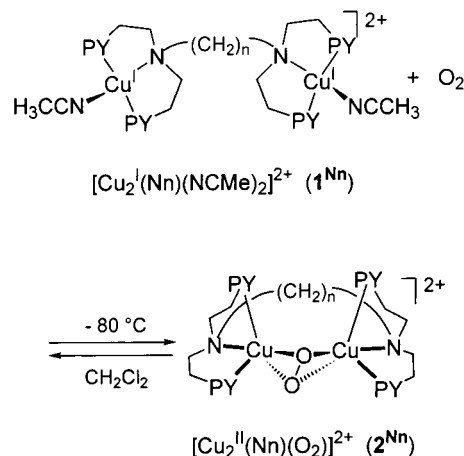
Complex	Resonance Raman $\nu(\text{O-O})$ and UV-vis
	765 cm^{-1} 365 nm 490 nm
	751 cm^{-1} 360 nm 458 nm
	741 cm^{-1} 360 nm 423 nm
	O-O: 730 cm^{-1} Cu ₂ (O) ₂ : 588 cm^{-1} 355 nm 405 (sh) nm
	745 cm^{-1} 360 nm 435 nm

Figure 1. Spectroscopic properties of dioxygen adducts $[\text{Cu}_2(\text{Nn})(\text{O}_2)]^{2+}$ (2^{Nn}), $\{(\text{MePY}_2\text{Cu})_2(\text{O}_2)\}^{2+}$ (**4**), and $[\text{Cu}_2(\text{NO}_2\text{-XYL-H})(\text{O}_2)]^{2+}$ (6^{NO_2}). The $\nu(\text{O-O})$ decreases from 2^{N_3} to 2^{N_5} within the 2^{Nn} series.

eties.^{4,33,34} Here, $[\text{Cu}_2(\text{R-XYL-H})]^{2+}$ (5^{R}) compounds react to form O_2 -adducts $[\text{Cu}_2(\text{R-XYL-H})(\text{O}_2)]^{2+}$ (6^{R}); for $[\text{Cu}_2(\text{NO}_2\text{-XYL-H})(\text{O}_2)]^{2+}$ (6^{NO_2}) UV-vis and resonance Raman spectroscopies reveal properties between those observed for 2^{N_4} and 2^{N_5} (see Figure 1).³⁴

The focus of this paper is a report on the kinetics-thermodynamics of O_2 -reaction with dicopper(I) complexes of Nn ($n = 3-5$), $[\text{Cu}_2^{\text{I}}(\text{Nn})(\text{MeCN})_2]^{2+}$ (1^{Nn}), Scheme 1. Reaction of O_2 with 1^{Nn} at 193 K (-80°C) in CH_2Cl_2 solvent affords adducts, $[\text{Cu}_2(\text{Nn})(\text{O}_2)]^{2+}$ (2^{Nn}), and these reactions are reversible in benchtop experiments, as demonstrated by the ability to remove O_2 from 2^{Nn} by application of a vacuum and carry out repetitive cycling of 2^{Nn} and 1^{Nn} .^{4,35,36} Dicopper(I) complexes 1^{Nn} also bind carbon monoxide (CO) reversibly.^{17,36}

Scheme 1



Kinetic measurements are desirable in order to (i) confirm the reversible nature of the O_2 -binding, (ii) deduce kinetic-thermodynamic parameters, and (iii) attempt to detect intermediates which might be observable on a faster time-scale, (i.e., milliseconds, for stopped-flow experiments). With the interesting structural and spectroscopic variations observed for the dioxygen adducts $[\text{Cu}_2(\text{Nn})(\text{O}_2)]^{2+}$ (2^{Nn}) (discussed above),²⁸ it is also worthwhile to compare and contrast their kinetic behavior.¹⁰

We have previously carried out low-temperature stopped-flow kinetic studies on other ligand-copper(I)/ O_2 reactions involving production of discrete spectroscopically or structurally well-characterized copper-dioxygen adducts, the first such measurements.¹⁰ These investigations have shed considerable light on fundamental aspects. Among these are that (i) superoxo-copper(II) intermediates ($\text{Cu}-\text{O}_2$) can be observed in systems utilizing tripodal tetradentate ligands (e.g., tmpa),^{10,37} (ii) in both $\text{Cu}-\text{O}_2$ and peroxodicopper(II) (Cu_2-O_2) products, dioxygen binding is strong (enthalpically), but room-temperature stability is generally precluded by highly unfavorable entropies of formation, (iii) binucleating analogues of mononuclear systems may increase reaction rates for formation of Cu_2-O_2 species, although they may or may not confer greater overall complex stability, and (iv) solvent/medium or ligand design effects can be dramatic, sometimes leading to near-room-temperature Cu_2-O_2 complex stability.^{10,38} The present investigation extends our previous studies to these complexes of Nn or MePY2 with tridentate coordination.

Experimental Section

Materials and Methods. The general preparative procedures and methods for characterization of ligands and complexes have been previously described.^{35,36} Improved ligand preparations are reported here. *Warning:* While we have experienced no problems in working with perchlorate compounds, they are potentially explosive, and care must be taken not to work with large quantities.

Synthesis of Ligands. N3. To 2-vinylpyridine (20 g, 0.19 mol, purified by passing through a short silica column with diethyl ether as the eluent, followed by removal of ether by rotary evaporation) in a 200-mL round-bottom flask was added 1,3-diaminopropane (1.406 g, 0.019 mol) along with 2 drops of glacial acetic acid and a magnetic stir bar. The initial solution was a clear, golden color. After stirring and heating to $82-84^\circ\text{C}$, the solution became dark brown and visibly more viscous after a day. (Heating the solution to higher temperatures

(33) Karlin, K. D.; Nasir, M. S.; Cohen, B. I.; Cruse, R. W.; Kaderli, S.; Zuberbühler, A. D. *J. Am. Chem. Soc.* **1994**, *116*, 1324-1336.

(34) Pidcock, E.; Obias, H. V.; Zhang, C. X.; Karlin, K. D.; Solomon, E. I. *J. Am. Chem. Soc.* **1998**, *120*, 7841-7847.

(35) Karlin, K. D.; Haka, M. S.; Cruse, R. W.; Meyer, G. J.; Farooq, A.; Gultneh, Y.; Hayes, J. C.; Zubieta, J. *J. Am. Chem. Soc.* **1988**, *110*, 1196-1207.

(36) Karlin, K. D.; Tyeklár, Z.; Farooq, A.; Haka, M. S.; Ghosh, P.; Cruse, R. W.; Gultneh, Y.; Hayes, J. C.; Toscano, P. J.; Zubieta, J. *Inorg. Chem.* **1992**, *31*, 1436-1451.

(37) Karlin, K. D.; Wei, N.; Jung, B.; Kaderli, S.; Niklaus, P.; Zuberbühler, A. D. *J. Am. Chem. Soc.* **1993**, *115*, 9506-9514.

(38) Karlin, K. D.; Lee, D.-H.; Kaderli, S.; Zuberbühler, A. D. *Chem. Commun.* **1997**, 475-476.

may result in undesirable polymerization of 2-vinylpyridine.) The reaction was deemed complete after 5 days by monitoring the crude mixture using TLC. The excess 2-vinylpyridine was then removed by using a high vacuum rotary evaporator. Purification of the crude product in several batches on silica gel using 98% CH₃OH–2% NH₄OH gives a yellow solid, which is then extracted with ethyl acetate to remove the dissolved silica. The solvent is then removed by rotary evaporation to yield 5.828 g of the pure, yellow oily product (62% based on diamine).

N4. The synthesis of N4 follows the analogous procedure as that for N3, except that typically, only 2 days of heating at 82–84 °C were needed for the reaction to go to completion as determined by TLC. The yield of the pure, dark yellow solid product (it is initially an oily product but becomes a solid upon storage in the freezer) is typically 80–90% based on the diamine starting material.

N5. The synthesis of N5 follows the analogous procedure as that for N3, and the reaction typically takes 4–5 days of heating at 82–84 °C. The yield of the pure, yellow oily product is typically 70–75% based on the diamine.

[Cu(MeCN)₄][ClO₄]. To 100 mL of CH₃CN in a 200-mL Erlenmeyer flask, were added Cu^{II}(ClO₄)₂·6H₂O (5 g, 0.0135 mol) along with a magnetic stir bar. An excess of copper metal in pellet form (3.4 g, 0.054 mol) then was added, and the reaction mixture was stirred for 4 h at room temperature at 25 °C. The solution changed slowly from blue to gray over the course of 4 h. The solution then was filtered using a medium porosity frit, and the filtrate was concentrated by vacuum to ~40 mL. Diethyl ether (~50 mL) was then added slowly to the filtrate, and the solution was placed in the freezer (0 °C) to yield white needle crystals overnight (6.526 g, 74% yield). Anal. Calcd for (C₈H₁₂N₄ClCuO₄): C, 29.37; H, 3.70; N, 17.12. Found: C, 29.61; H, 3.67; N, 16.89.

[Cu₂(N5)(MeCN)₂][ClO₄]₂ (1^{N5}). Under an Ar atmosphere, N5 (0.100 g, 0.000191 mol) in ~15 mL of CH₃CN was added with stirring to solid [Cu(MeCN)₄][ClO₄] (0.125 g, 0.000382 mol). The resulting golden yellow solution was allowed to stir for 30 min. Addition of 30 mL of diethyl ether afforded a bright yellow precipitate, which was collected by filtration under Ar. Recrystallization with dichloromethane/diethyl ether (5 mL:10 mL) at 0 °C produced 0.136 g (76%) of yellow microcrystalline material. Anal. Calcd for (C₃₇H₄₈Cl₂Cu₂N₅O₈): C, 47.74; H, 5.20; N, 12.04. Found: C, 47.38, H, 5.04; N, 11.87. ¹H NMR (CD₃NO₂): δ 8.8–8.6 (4 H, py-6, br s), 8.0–7.8 (4 H, py-4, br s), 7.60–7.2 (8 H, py-3, py-5, br d), 3.3–3.1 (8 H, s), 3.1–2.8 (8 H, br s), 2.6–2.4 (4 H, s), 2.1–1.9 (6 H, CH₃CN, s), 1.4–1.2 (4 H, s), 1.2–1.0 (2 H, s).

[Cu(MePY2)(MeCN)][ClO₄]-CH₂Cl₂ (3). Under an Ar atmosphere, MePY2 (0.083 g, 0.00034 mol) in ~10 mL of CH₂Cl₂ was added with stirring to solid [Cu(MeCN)₄][ClO₄] (0.113 g, 0.00034 mol). The resulting golden yellow solution was allowed to stir for 30 min at room temperature (rt), and then ~20 mL of diethyl ether was added to produce a cloudy solution. The resulting solution was left to stand under Ar at –30 °C for 2 h, after which a yellow precipitate formed. The solvent was then decanted under Ar flow, and the yellow solid was washed with degassed diethyl ether (2 × 20 mL) and dried in vacuo to yield 0.127 g (83%) of a light yellow powder. Anal. Calcd for (C₁₈H₃₀Cl₃-CuN₄O₄): C, 43.09; H, 4.75; N, 11.48. Found: C, 43.08; H, 4.72; N, 11.49. ¹H NMR (CD₃NO₂): δ 8.8–8.6 (2 H, py-6, br s), 8.0–7.8 (2 H, py-4, m), 7.6–7.4 (4 H, py-3, py-5, m), 5.32 (2 H, CH₂Cl₂), 3.3–3.1 (4 H, s), 3.1–2.8 (4 H, br s), 2.5–2.3 (3 H, s), 2.1–1.9 (3 H, CH₃CN, s).

Stopped-Flow Experiments. Rapid kinetics were followed using a SF-21 variable-temperature stopped-flow unit (Hi-Tech Scientific) combined with a TIDAS-16 HQ/UV–Vis 512/16B diode array spectrometer (J & M, 507 diodes, 300–720 nm, 1.3 ms minimum sampling time). Data acquisition (up to 256 complete spectra, up to 4 different time bases) was done based on the Kinspec program (J & M). For numerical analysis, all data were pretreated by factor analysis and concentration profiles based on various kinetic models were calculated by numerical integration using either Specfit (Spectrum Software Ass.) or Globfit (MATLAB).³⁹ The solvent CH₂Cl₂ (Uvasol,

Merck) was dried using CaH₂ and redistilled under vacuum immediately prior to use. Thermal expansion of the solvent was taken into account. Initial oxygen concentration was 1.895 mM for all systems studied. For further details see ref 37. For [Cu₂(N3)(MeCN)₂](ClO₄)₂ (1^{N3}), four series of Cu(I) concentrations were used to carry out a total of 193 measurements between –90 and +22 °C. Of these, 81 were used for the final analysis. The concentrations of Cu(I) solutions used were 0.362 mM, 0.168 mM, 0.141 mM, and 0.0761 mM. Reaction times measured ranged from 3 to 212 s. For [Cu₂(N4)(MeCN)₂](ClO₄)₂ (1^{N4}), three series of Cu(I) concentrations were used to carry out a total of 175 measurements between –90 and +10 °C. Of these, 84 were used for the final analysis. The concentrations of Cu(I) solutions used were 0.527 mM, 0.284 mM, and 0.137 mM. Reaction times measured ranged from 0.3 to 230 s. For [Cu₂(N5)(MeCN)₂](ClO₄)₂ (1^{N5}), three series of Cu(I) concentrations were used to carry out a total of 163 measurements between –90 and +20 °C. A 418-nm filter was used to reduce possible photochemical contributions. Of these, 121 were used for the final analysis. The concentrations of Cu(I) solutions used were 0.328 mM, 0.219 mM, and 0.0790 mM. Reaction times measured ranged from 41 to 201 s. For [(MePY2)Cu(MeCN)](ClO₄) (3), five solutions with the same concentration of Cu(I) complex (2.54 mM) were prepared in a glovebox. After adding 0, 0.5, 1, 2, and 4 equiv of MeCN ([MeCN] = 0, 1.30, 2.64, 5.19, and 10.55 mM), a total of 16 measurements at –30 °C have been carried out. The reaction time measured was 300 s throughout.

Results and Discussion

Ligands and Complexes. We have previously described the synthesis of N3, N4, and N5 binucleating ligands in one-step procedures starting from commercially available compounds.^{35,36} Procedures that lead to improved yields utilizing shorter reaction times are described in this report (see Experimental Section). Our previous publications also describe the syntheses of several types of dicopper(I) complexes with the Nn ligands, including bis-hexafluorophosphate and/or bis-perchlorate salts of three-coordinate complexes, [Cu₂(Nn)]²⁺.^{35,36} Three-coordinate copper(I) species readily form four-coordinate adducts, and carbon monoxide containing complexes, [Cu₂(Nn)(CO)₂]²⁺, and acetonitrile adducts, [Cu₂(Nn)(MeCN)₂]²⁺ (1^{Nn}) have been characterized. The acetonitrile adducts are the focus of the present kinetic study, as they can be more readily prepared as stable (but of course oxygen-sensitive) compounds with good shelf life. Perchlorate salts [Cu₂(Nn)(MeCN)₂](ClO₄)₂ (1^{Nn}-(ClO₄)₂) were chosen for the present study. Hexafluorophosphate salts were not favored, because fluoride abstraction reactions are sometimes observed resulting in fluoride-bridged dicopper(II) complexes.^{29,40} The 1^{Nn}-(ClO₄)₂ complexes are soluble in dichloromethane, even at low temperatures (e.g., (183 K; –90 °C), and they react rapidly with dioxygen. The complex with N5, 1^{N5}-(ClO₄)₂ had not been previously described, and its synthesis is reported here (Experimental Section). As it turns out, the presence of acetonitrile, even 1 equiv per cuprous ion in [Cu^I₂(Nn)(MeCN)₂]²⁺ (1^{Nn}), has a noticeable effect upon the kinetics of O₂-binding. This will be discussed further below.

Mechanism of Oxygenation of Previously Studied Related Xyllyl Complexes, [Cu₂(R-XYL-H)(O₂)]²⁺ (6^R). Because of the close similarity of the ligand architecture, previous investigations and results on the formation of dioxygen complexes 6^R are relevant as a starting point and basis for comparison in the present investigation. As mentioned in the Introduction, compounds [Cu₂(R-XYL-H)]²⁺ (5^R) react to form O₂-adducts (μ-η²-η²-peroxo-dicopper(II) species) [Cu₂(R-XYL-H)(O₂)]²⁺ (6^R). The kinetic studies indicate that the oxygenation of 5^R is reversible, and best described by a simple one-step equilibrium

(39) Neuhold, Y.-M.; Ph.D. Dissertation, University of Basel, 1999.

(40) Jacobson, R. R.; Tyeklár, Z.; Karlin, K. D.; Zubieta, J. *Inorg. Chem.* **1991**, *30*, 2035–2040.

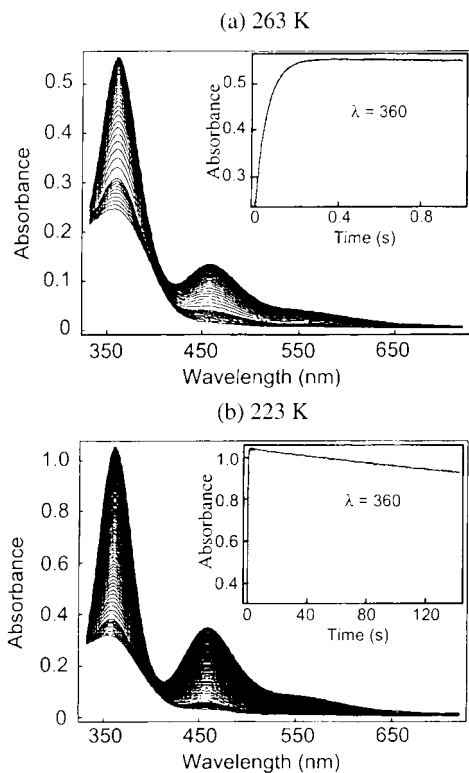
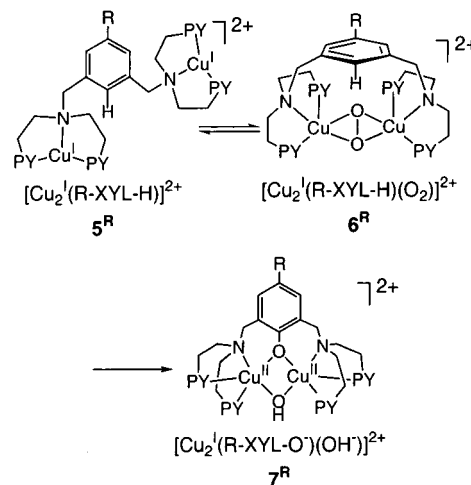


Figure 2. Stopped-flow spectrophotometric monitoring of the evolution of peroxo complex $[\text{Cu}_2(\text{N}4)(\text{O}_2)]^{2+}$ ($2^{\text{N}4}$) in CH_2Cl_2 at (a) 263 K and (b) 223 K. Inset: absorbance vs time at 360 nm based on model described in Scheme 3. $[\text{O}_2] = 1.9 \times 10^{-3}$ M. See text for further explanation.

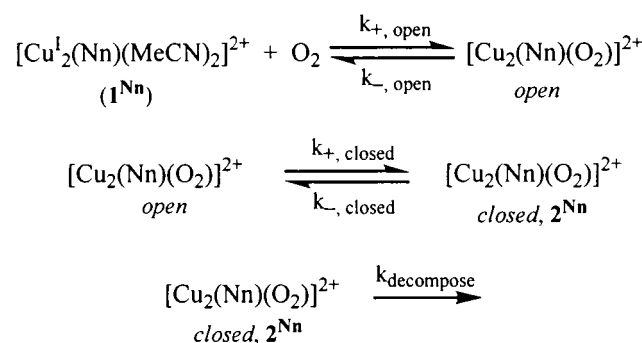
process, Scheme 2. No intermediates, such as $\text{Cu}-\text{O}_2$ $\text{Cu}(\text{II})$ -superoxo species,⁴¹ were observed in the stopped-flow kinetic experiments. It is notable that 6^{R} complexes further react in an arene hydroxylation reaction (Scheme 2) to give phenoxo and hydroxo-bridged dicopper(II) complexes $[\text{Cu}_2(\text{R-XYL-O}^-)(\text{OH})]^{2+}$ (7^{R}), and investigations of these reactions and those of analogues led to a detailed mechanistic picture of that process involving “activation” of O_2 and model enzyme monooxygenase reactivity.^{4,34,37}

Oxygenation Behavior of $[\text{Cu}_2^{\text{I}}(\text{Nn})(\text{MeCN})_2]^{2+}$ (1^{Nn}), Basic Observations. The previous stopped-flow investigations carried out on xylyl systems, $[\text{Cu}_2(\text{R-XYL-H})]^{2+}$ (5^{R}), were normally carried out in dichloromethane as solvent (and as bis- PF_6^- salts). As CH_2Cl_2 had been a good solvent for these systems, this was continued in the present study for 1^{Nn} . Figure 2a shows the UV-vis behavior when, for example, $[\text{Cu}_2^{\text{I}}(\text{N}4)(\text{MeCN})_2]^{2+}$ ($1^{\text{N}4}$) reacts with an excess of O_2 (i.e., saturated solutions; pseudo-first-order conditions) at 263 K (-10°C). The major features of the UV-vis spectrum observed in benchtop monitoring of this reaction³⁵ are observed, with formation of an intense absorption at 360 nm, and vis peak at 458 nm, these being the characteristic features of $[\text{Cu}_2(\text{N}4)(\text{O}_2)]^{2+}$ ($2^{\text{N}4}$), with μ - η^2 : η^2 -peroxo-dicopper(II) core. The inset of Figure 2a shows the absorbance versus time trace at 360 nm, and the maximum concentration of $2^{\text{N}4}$ at this temperature and complex concentration ($\sim 10^{-4}$ M) occurs by ~ 0.3 s. No intermediates are observed and full buildup of oxygenated complex $2^{\text{N}4}$ does not occur at this relatively high temperature. At a lower temperature of 223

Scheme 2



Scheme 3



K (Figure 2b), a much larger proportion of $1^{\text{N}4}$ is oxygenated to $2^{\text{N}4}$, as can be seen by the relative absorbance changes in Figure 2b compared to Figure 2a. The inset of Figure 2b shows that in the longer time frame of that particular experiment (> 100 s), decomposition of $[\text{Cu}_2(\text{N}4)(\text{O}_2)]^{2+}$ ($2^{\text{N}4}$) occurs at this temperature, in accord with benchtop UV-vis monitoring of the chemistry (where such decomposition is accompanied by loss of intensity of the charge-transfer bands). The $[\text{Cu}_2(\text{Nn})(\text{O}_2)]^{2+}$ (2^{Nn}) dioxygen adducts are stable for hours at lower temperatures, i.e., 193 K (-80°C) in CH_2Cl_2 solvent. Thus, these observations and the data analyses, described more fully below, lead to the kinetic mechanisms described by the equations in Scheme 3.

Analysis of Higher Temperature Data (253 to 283 K). As described in previous publications,^{10,33,37,42} the variable-temperature multiwavelength stopped-flow data have been analyzed by global (factor) analysis. The data from both the higher (253 to 283 K) and lower (213 to 233 K) temperature regimes can be successfully analyzed by using the equations described in Scheme 3. In our model, the dicopper(I) complexes $[\text{Cu}_2^{\text{I}}(\text{Nn})(\text{MeCN})_2]^{2+}$ (1^{Nn}) first react with O_2 reversibly ($k_{+, \text{open}}$ and $k_{-, \text{open}}$) to form an “open” copper-dioxygen adduct, presumably a superoxo complex, which we do not detect spectroscopically. The “open” compound then undergoes another reversible step ($k_{+, \text{closed}}$ and $k_{-, \text{closed}}$) to form the peroxo compound, $[\text{Cu}_2(\text{Nn})(\text{O}_2)]^{2+}$ (2^{Nn}), which then decomposes in an irreversible step, $k_{\text{decompose}}$. In the higher temperature range, the reverse reaction of $[\text{Cu}_2(\text{Nn})(\text{O}_2)]^{2+}$ (2^{Nn}) to the open form ($k_{-, \text{closed}}$) occurs at

(41) For the tetradentate ligand tmpa and a for a quinolyl analogue, mononuclear copper(II)-superoxo intermediates have been detected in stopped-flow experiments, and their kinetic behavior described quantitatively (see refs 10 and 37).

(42) Mahapatra, S.; Kaderli, S.; Llobet, A.; Neuhold, Y.-M.; Palanché, T.; Halfen, J. A.; Young Jr., V. G.; Kaden, T. A.; Que, L., Jr.; Zuberbühler, A. D.; Tolman, W. B. *Inorg. Chem.* **1997**, *36*, 6343–6356.

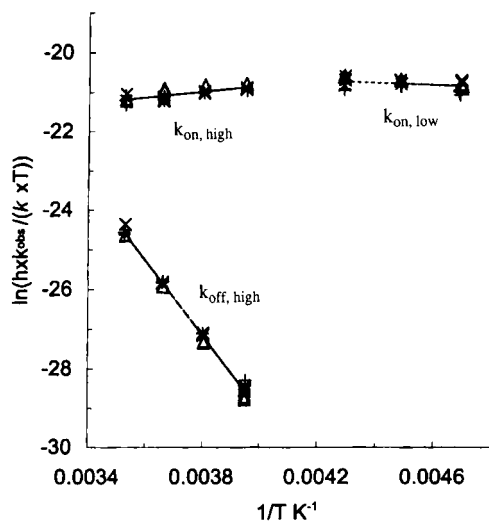


Figure 3. Eyring plots for $k_{\text{on,high}}$, $k_{\text{off,high}}$, and $k_{\text{on,low}}$ pertaining to the formation of $[\text{Cu}_2(\text{N4})(\text{O}_2)]^{2+}$ (2^{N4}) from $[\text{Cu}_2(\text{N4})(\text{MeCN})_2][\text{ClO}_4]_2$ (1^{N4}): k , Boltzmann constant; h , Planck constant; $[\text{O}_2] = 1.9 \times 10^{-3}$ M; (—) high-temperature regime, 253–283 K; (···) low-temperature regime, 213–233 K. $[1^{\text{N4}}] = 1.37 \times 10^{-4}$ M (x), 2.84×10^{-4} M (+), and 5.27×10^{-4} M (Δ). See text.

a significant rate, unlike at the lower temperatures (vide infra). Therefore, based on the fact that we do not detect an intermediate (i.e., the open form does not accumulate at higher temperatures), the forward reaction of $[\text{Cu}_2(\text{Nn})(\text{MeCN})_2]^{2+}$ (1^{Nn}) to form $[\text{Cu}_2(\text{Nn})(\text{O}_2)]^{2+}$ open ($k_{+, \text{open}}$) cannot be the rate determining step at higher temperatures and the first step ($1^{\text{Nn}} + \text{O}_2$) is a left-lying equilibrium. The rate-determining step in the higher temperature regime therefore is associated with a rate constant of $k_{\text{on,high}} = (k_{+, \text{open}}/k_{-, \text{open}})(k_{+, \text{closed}})$.

From the variable-temperature data, Eyring plots for both $k_{\text{on,high}}$ and $k_{\text{off,high}}$ ($k_{\text{on,high}} = (k_{+, \text{open}}/k_{-, \text{open}})(k_{+, \text{closed}})$; $k_{\text{off,high}} = k_{-, \text{closed}}$) have been obtained and are given in Figure 3 (data for 1^{N3} and 1^{N5} are analogous and given in the Supporting Information). The derived kinetic and thermodynamic parameters are summarized in Table 1, with calculated rate and equilibrium constants given for 183, 223, and 298 K. The overall formation of $[\text{Cu}_2(\text{Nn})(\text{O}_2)]^{2+}$ (2^{Nn}) occur rapidly, with $k_{\text{on,high}} \approx 10^3 \text{ M}^{-1} \text{ s}^{-1}$ (calculated) at room temperature, Table 1. $[\text{Cu}_2(\text{Nn})(\text{O}_2)]^{2+}$ (2^{Nn}) form with zero to negative activation enthalpies ($\Delta H^\ddagger = 0$ to -11 kJ mol^{-1}), indicating that their formation is not an elementary step, consistent with the occurrence of a preequilibrium. The same phenomenon is observed and has been discussed for the formation of the analogue xylyl complexes $[\text{Cu}_2(\text{R-XYL-H})(\text{O}_2)]^{2+}$ (6^{R}).^{4,10,33} The preequilibrium probably involves O_2 -binding to one of the two coppers in $[\text{Cu}_2(\text{Nn})(\text{MeCN})_2]^{2+}$ (1^{Nn}) or in an acetonitrile dissociated species $[\text{Cu}_2(\text{Nn})]^{2+}$, i.e., formation of a $\text{Cu}(\text{II})$ -superoxo intermediate $\text{Cu}(\text{I})\cdots\text{Cu}(\text{II})-\text{O}_2^-$, which does not build up in concentration (i.e., left-lying equilibrium) and is therefore not spectroscopically observable. Such a process would seem to be necessary in any case, since one would not expect O_2 to simultaneously bind both copper ions in the dicopper complex of Nn. The relatively large negative activation entropies ($\Delta S^\ddagger = -177$ to $-217 \text{ K}^{-1} \text{ mol}^{-1}$) for formation of $[\text{Cu}_2(\text{Nn})(\text{O}_2)]^{2+}$ (2^{Nn}) fall in line with those values observed for $[\text{Cu}_2(\text{R-XYL-H})(\text{O}_2)]^{2+}$ (6^{R}) complexes (where ΔS^\ddagger vary from -66 to $-167 \text{ J K}^{-1} \text{ mol}^{-1}$), reflective of the ordering in the transition state, typical for dioxygen binding. Since the dicopper(I) complexes $[\text{Cu}_2(\text{R-XYL-H})]^{2+}$ (5^{R}) do not possess MeCN ligands whose dissociation might make ΔS^\ddagger less negative, and we have a roughly comparable ΔS^\ddagger value here for the Nn complexes, then one

might conclude that since MeCN dissociation is facile (at these temperatures), that it is relatively unimportant in its contribution to the kinetic parameters observed for O_2 -binding to 1^{Nn} . Another possible explanation is that O_2 -binding to 1^{Nn} is an associative process (i.e., no initial loss of MeCN ligands).

Lower Temperature Regime (213 to 233 K). As one goes to lower temperature, the rate determining step in the formation of $[\text{Cu}_2(\text{Nn})(\text{O}_2)]^{2+}$ (2^{Nn}), Scheme 3, differs from that at the higher temperatures. This is due to the very strong binding of dioxygen to 1^{Nn} at these reduced temperatures (213 to 233 K; -40 to -60 °C), which are thus accompanied by immeasurable off rates, $k_{-, \text{closed}}$ (i.e., Cu_n-O_2 bond cleavage and O_2 dissociation). As a result, at lower temperatures, the formation of $[\text{Cu}_2(\text{Nn})(\text{O}_2)]^{2+}$ open ($k_{+, \text{open}}$) becomes rate determining and will be referred to as $k_{\text{on,low}}$. Thus, as Figure 3 shows, the Eyring plots of the oxygenation of $[\text{Cu}_2(\text{N4})(\text{MeCN})_2]^{2+}$ (1^{N4}) (data for 1^{N3} and 1^{N5} are in the Supporting Information) give somewhat different slopes for the high versus low temperature regimes. Still, these calculated low-temperature O_2 -binding rates (Table 1) are quite comparable to those obtained from the kinetic fittings from the higher temperature data (i.e., Eyring plot of $k_{\text{on,high}}$). It is notable that very low (near zero) enthalpies of activation for $k_{\text{on,low}}$ are observed ($\Delta H^\ddagger = 2.5$ to 10 kJ mol^{-1}), still suggesting a preequilibrium step or steps. Thus, the overall binding of O_2 to $[\text{Cu}_2(\text{Nn})(\text{MeCN})_2]^{2+}$ (1^{Nn}) appears to involve several reactions, perhaps including dissociation of nitrile (MeCN) ligands (especially at lower temperatures), formation and rearrangement of different Cu_n-O_2 structural types, or all of the above. The lack of formation of a spectroscopically distinct intermediate which might be characterized precludes further insights or conclusions.

Oxygenation of $[\text{Cu}_2(\text{Nn})(\text{MeCN})_2]^{2+}$ (1^{Nn}) Below 213 K. Unusual Kinetic Behavior. Below this temperature, the dioxygen adduct $[\text{Cu}_2(\text{Nn})(\text{O}_2)]^{2+}$ (2^{Nn}) still forms upon oxygenation. However, the kinetic behavior is complicated and not amenable to full analysis. Important primary observations are that when carrying out kinetic runs as a function of concentration, we observe that the rate of formation of 2^{Nn} decreases with increasing dicopper(I) (1^{Nn}) concentration, not in line with a first-order process.

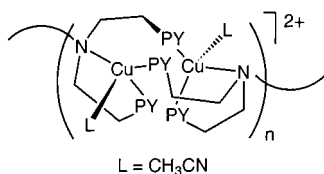
The explanation we favor for this lowest temperature kinetic behavior, described further below, is that oligomers of $[\text{Cu}_2(\text{Nn})(\text{MeCN})_2]^{2+}$ (1^{Nn}) tend to form. Straightforwardly, this could explain the concentration dependence observed, since breakup of the oligomers is required to form the binuclear intramolecular peroxo-dicopper(II) complex $[\text{Cu}_2(\text{Nn})(\text{O}_2)]^{2+}$ (2^{Nn}). Again, no intermediates were observable in these very low-temperature kinetic measurements, so no further insights into the course of oxygenation can be provided. For the complexes $[\text{Cu}_2(\text{Nn})(\text{MeCN})_2]^{2+}$ (1^{Nn}), what probably takes place is that one nitrogen donor of the Nn ligand (e.g., a pyridyl group) binds in an *intermolecular* fashion to a copper(I) ion which originates from a second molecule, instead of coordinating to the copper ion of its own chelate. This also occurs for the corresponding pyridyl donor originated from the ligand on the second copper, resulting in an oligomeric structure (see diagram). The MeCN present may or may not additionally ligate to the three-coordinated copper(I) ions.

There are many literature examples of this phenomenon, including copper(I) complexes employing tri or tetradentate nitrogen-containing chelates, such as tris-alkyl substituted pyrazolylborates,^{20,43,44} a tris-imidazolylmethoxymethane ligand,⁴⁵

(43) Mealli, C.; Arcus, C. A.; Wilkinson, J. L.; Marks, T. J.; Ibers, J. A. *J. Am. Chem. Soc.* **1976**, *98*, 711–718.

Table 1. Kinetic and Thermodynamic Parameters of N3, N4, and N5 Dicopper(I) Oxygenation

parameter	T (K)	1 ^{N3}	1 ^{N4}	1 ^{N5}
$k_{\text{on,low}}$ ($\text{M}^{-1} \text{s}^{-1}$)	183	$(1.1 \pm 0.1) \times 10^3$	$(2.5 \pm 0.3) \times 10^3$	$(4.1 \pm 0.3) \times 10^3$
	223	$(4.3 \pm 0.2) \times 10^3$	$(4.2 \pm 0.1) \times 10^3$	$(7.7 \pm 0.4) \times 10^3$
	298	$(2.3 \pm 0.3) \times 10^4$	$(8 \pm 1) \times 10^3$	$(1.7 \pm 0.3) \times 10^4$
ΔH^\ddagger (kJ mol^{-1})		10 ± 1	2.5 ± 0.9	3.6 ± 0.8
ΔS^\ddagger ($\text{J K}^{-1} \text{mol}^{-1}$)		-128 ± 7	-162 ± 4	-152 ± 4
$k_{\text{on,high}}$ ($\text{M}^{-1} \text{s}^{-1}$)	183	$(2.2 \pm 0.5) \times 10^3$	$(10 \pm 1) \times 10^3$	$(2.8 \pm 0.3) \times 10^4$
	223	$(2.6 \pm 0.2) \times 10^3$	$(5.7 \pm 0.4) \times 10^3$	$(9.0 \pm 0.4) \times 10^3$
	298	$(3.5 \pm 0.5) \times 10^3$	$(3.3 \pm 0.1) \times 10^3$	$(2.6 \pm 0.1) \times 10^3$
ΔH^\ddagger (kJ mol^{-1})		0 ± 3	-6.1 ± 0.8	-11.2 ± 0.5
ΔS^\ddagger ($\text{J K}^{-1} \text{mol}^{-1}$)		-177 ± 12	-198 ± 3	-217 ± 2
$k_{\text{off,high}}$ (s^{-1})	183	$(7.5 \pm 3.3) \times 10^{-6}$	$(1.2 \pm 0.3) \times 10^{-6}$	$(5 \pm 3) \times 10^{-7}$
	223	$(1.8 \pm 0.2) \times 10^{-1}$	$(1.4 \pm 0.1) \times 10^{-2}$	$(2.3 \pm 0.6) \times 10^{-3}$
	298	$(2.2 \pm 0.5) \times 10^4$	$(7.6 \pm 0.4) \times 10^2$	$(4.2 \pm 0.3) \times 10^1$
ΔH^\ddagger (kJ mol^{-1})		84 ± 5	78 ± 1	70 ± 4
ΔS^\ddagger ($\text{J K}^{-1} \text{mol}^{-1}$)		120 ± 18	72 ± 4	21 ± 15
K_1 (M^{-1}) (= $k_{\text{on,high}}/k_{\text{off,high}}$)	183	$(3 \pm 1) \times 10^8$	$(8 \pm 2) \times 10^9$	$(5 \pm 3) \times 10^{10}$
	223	$(1.5 \pm 0.2) \times 10^4$	$(3.7 \pm 0.4) \times 10^5$	$(3.5 \pm 0.9) \times 10^6$
	298	$(1.6 \pm 0.4) \times 10^{-1}$	4.2 ± 0.3	$(5.8 \pm 0.5) \times 10^1$
ΔH° (kJ mol^{-1})		-84 ± 6	-84 ± 1	-81 ± 4
ΔS° ($\text{J K}^{-1} \text{mol}^{-1}$)		-297 ± 22	-270 ± 5	-238 ± 15



tripodal tetradentates with oxazoline⁴⁶ or pyridyl-amine⁴⁷ donors, and others.^{48–51} Cu(I)–Cu(I) interactions,^{49–51} or aromatic π -stacking⁵² (e.g., pyridyl groups)⁴⁷ appear to facilitate the formation or stabilization of such dimer (oligomer) structures. X-ray structures are known for all but one of the cited examples.⁵³

In summary, the poorly defined and complicated kinetics of $[\text{Cu}_2(\text{Nn})(\text{MeCN})_2]^{2+}$ (**1**^{Nn}) reaction with dioxygen at the lowest temperatures (i.e., below ~ 213 K) is rationalized by the oligomerization which we propose. Low-temperature NMR spectroscopy of **1**^{N4} in dichloromethane reveals only a general broadening of most signals, so dynamic solution behavior, which is common for copper(I) chelates with nitrogenous ligands,^{16,43,44,54} clearly occurs, but is not fully interpretable.⁵⁵ We recently noted

that the lowest-temperature kinetic behavior of $[\text{Cu}_2(\text{H-XYL-H})]^{2+}$ (**5**^H) in acetone was complicated, possibly also for similar reasons.⁵⁶ We also feel that the presence of only one MeCN molecule per copper ion in $[\text{Cu}_2(\text{Nn})(\text{MeCN})_2]^{2+}$ (**1**^{Nn}) helps to promote oligomerization; in other words, additional or excess MeCN might favor an equilibrium where tetracoordination for copper(I) includes the nitrile and thus frees up binuclear species $[\text{Cu}_2(\text{Nn})(\text{MeCN})_2]^{2+}$ (**1**^{Nn}), which would have the expected kinetic behavior.

Comparison and Comment on Kinetics of Oxygenation of $[\text{Cu}_2(\text{N4})(\text{PF}_6)_2$. We previously⁵⁷ published preliminary kinetic observations on the oxygenation behavior of $[\text{Cu}_2(\text{N4})](\text{PF}_6)_2$, that N4 complex possessing *no* MeCN ligands, and with hexafluorophosphate counteranions. Unlike in the present study employing MeCN adduct $[\text{Cu}_2(\text{N4})(\text{MeCN})_2]^{2+}$ (**1**^{N4}), for $[\text{Cu}_2(\text{N4})(\text{PF}_6)_2$ at the lowest temperatures, a copper–dioxygen adduct intermediate *was* in fact detected prior to its conversion to the usual final product (at reduced temperatures), the μ - η^2 - η^2 -peroxo complex $[\text{Cu}_2(\text{N4})(\text{O}_2)]^{2+}$ (**2**^{N4}) with λ_{max} 360 and 458 nm. On the basis of the above discussion of unusual behavior at low temperatures ascribed to copper(I) complex oligomer formation, it is likely that the previous study also involved oxygenation of oligomers, which however then led to an O₂-intermediate at those lowest temperatures. We can rule out that the counterion is the most important factor in this effect,⁵⁸ and thus the absence of one MeCN per Cu is implicated as critical for the (spectroscopic) observation of a copper-dioxygen intermediate. We again suggest that the presence of MeCN and its strong coordination to copper(I) helps the breakup of oligomers forming at low temperatures; conversely, the absence of MeCN thus permits oligomer formation. Further investigations are required for complexes possessing no MeCN,⁵⁹ and these are in progress. In the present study, below, we illustrate the effect of MeCN on the kinetics of reaction of mononuclear complex $[(\text{MePY}_2)\text{Cu}^+(\text{MeCN})]^+$ (**3**), which is compared in its behavior with the binuclear Nn series of

(44) Carrier, S. M.; Ruggiero, C. E.; Houser, R. P.; Tolman, W. B. *Inorg. Chem.* **1993**, *32*, 4889–4899.

(45) Sorrell, T. N.; Borovik, A. S. *J. Am. Chem. Soc.* **1987**, *109*, 4255–4260.

(46) Sorrell, T. N.; Pigge, F. C.; White, P. S. *Inorg. Chim. Acta* **1993**, *210*, 87–90.

(47) Wei, N.; Murthy, N. N.; Tyeklár, Z.; Karlin, K. D. *Inorg. Chem.* **1994**, *33*, 1177–1183.

(48) Drew, M. G. B.; Lavery, A.; McKee, V.; Nelson, S. M. *J. Chem. Soc., Dalton Trans.* **1985**, 1771–1774.

(49) Gagne, R. R.; Kreh, R. P.; Dodge, J. A.; Marsh, R. E.; McCool, M. *Inorg. Chem.* **1982**, *21*, 254–261.

(50) Singh, K.; Long, J. R.; Stavropoulos, P. *Inorg. Chem.* **1998**, *37*, 1073–1079.

(51) Lee, S. W.; Trogler, W. C. *Inorg. Chem.* **1990**, *29*, 1659–1662.

(52) Bonnefous, C.; Bellec, N.; Thummel, R. P. *Chem. Commun.* **1999**, 1243–1244.

(53) It is interesting to note that some of the structures show that in the dimer form of these complexes, one atom of a chelate may remain uncoordinated in the copper(I) dimer structure. For instance, a potentially tetradentate ligand becomes tridentate or a potentially tridentate ligand becomes bidentate (see ref 44).

(54) Coggin, D. K.; Gonzalez, J. A.; Kook, A. M.; Stanbury, D. M.; Wilson, L. *J. Inorg. Chem.* **1991**, *30*, 1115–1125.

(55) The two methylene signals for the two chemically distinct $-\text{CH}_2-$ groups between the pyridyl donors and tertiary amine of N4, actually broaden and begin to coalesce upon lowering the temperature from 308 to 183 K. Thus, dynamic behavior is occurring, but full analysis is not possible.

(56) Becker, M.; Schindler, S.; Karlin, K. D.; Kaden, T. A.; Kaderli, S.; Palanche, T.; Zuberbühler, A. D. *Inorg. Chem.* **1999**, *38*, 1989–1995.

(57) Jung, B.; Karlin, K. D.; Zuberbühler, A. D. *J. Am. Chem. Soc.* **1996**, *118*, 3763–3764.

(58) Unpublished observations.

(59) We think it likely that the previous kinetics study on $[\text{Cu}_2(\text{N4})](\text{PF}_6)_2$ involved samples which contained traces of MeCN, influencing the observations. Currently, we are synthesizing samples which will have absolutely no MeCN for further investigations.

Table 2. Kinetics-Thermodynamic Comparisons of O₂-Reaction of Binuclear Copper(I) Complexes

complexes ^a	ΔH^\ddagger (kJ mol ⁻¹)	ΔS^\ddagger (J K ⁻¹ mol ⁻¹)	k_{on} 223 K (M ⁻¹ s ⁻¹)	ΔH° (kJ mol ⁻¹)	ΔS° (J K ⁻¹ mol ⁻¹)	refs
1^{Nn} high temp	-11 to 0	-177 to -217	2.6–9.0 × 10 ³	-81 to -84	-238 to -297	this study
1^{Nn} low temp	2.5 to 10	-128 to -162	4.3–7.7 × 10 ³			this study
XYL-H (acetone)	2.1 ± 0.7	-174 ± 3	1.58 × 10 ³ ^b	-42.3 ± 0.4	-176 ± 2	56
XYL-H (CH ₂ Cl ₂)	8.2 ± 0.1	-146 ± 1	1.30 × 10 ³	-62 ± 1	-196 ± 6	33, 60
[Cu ₂ (N4)] ²⁺	18 ± 2	-70 ± 9	(8 ± 2) × 10 ⁴	-58 ± 2	-165 ± 8	57
<i>m</i> -XYL ^{iPr4}	39.4 ± 0.5	-30 ± 2	77.3			42
<i>i</i> -Pr ₄ dtne	39.4 ± 0.1	-32.0 ± 0.4	58.8			42, 61

^a See text or footnotes for further compound description. ^b 253 K.

complexes, **1^{Nn}**. It is interesting to compare and contrast the equilibrium O₂-binding parameters for the present case, reaction of O₂ with [Cu₂(N4)(MeCN)₂]²⁺ (**1^{N4}**) to form [Cu₂(N4)(O₂)]²⁺ (**2^{N4}**), versus the reaction of [Cu₂(N4)](PF₆)₂ with dioxygen, forming the same product **2^{N4}**.⁵⁷ For formation of **2^{N4}** from **1^{N4}**, $\Delta H^\circ = -84 \pm 1$ kJ mol⁻¹ and $\Delta S^\circ = -270 \pm 5$ J K⁻¹ mol⁻¹, Table 1; K_1 values at various temperatures are also provided in Table 1. By contrast, the previously obtained equilibrium O₂-binding parameters for overall formation of **2^{N4}** from [Cu₂(N4)](PF₆)₂ were determined to be $\Delta H^\circ = -58 \pm 2$ kJ mol⁻¹ and $\Delta S^\circ = -165 \pm 8$ J K⁻¹ mol⁻¹ (Table 2). The difference in ΔH° (-84 versus -58 kJ mol⁻¹) is striking. Comparing actual K_1 values (Table 1) shows that at 183 K, K_1 is ~100 times greater for formation of **2^{N4}** from **1^{N4}**, but at 223 K, K_1 is about the same (10⁵–10⁶ M⁻¹) for both situations. It seems likely that those differences observed for thermodynamic parameters for these two situations involving formation of **2^{N4}** are significant, in reality reflecting strong differences in the starting point for the reactions, i.e., the more or less unknown structures of the dicopper(I) complexes (i.e., [Cu₂(N4)(MeCN)₂](ClO₄)₂ (**1^{N4}**-(ClO₄)₂) versus [Cu₂(N4)](PF₆)₂), as discrete binuclear complexes or oligomers or mixtures, etc.

Further Comparisons of Dicopper(I) Complex Reactions with O₂. The data show that for N3, N4 and N5 ligand complexes, formation of [Cu₂(Nn)(O₂)]²⁺ (**2^{Nn}**) from [Cu₂(Nn)(MeCN)₂]²⁺ (**1^{Nn}**) occurs in a remarkably similar fashion and that the rates, activation parameters, and thermodynamic constants are all relatively close to one another. However, some trends or observations may be worth noting. For example, ΔH^\ddagger values are all reduced for $k_{\text{on,high}}$ (zero or negative), compared to corresponding parameters for $k_{\text{on,low}}$ (2.5 to 10 kJ mol⁻¹), Tables 1 and 2. This is quite in line with previous observations that formation of the second copper–dioxygen bond has a lower activation enthalpy than breaking up the first one. The low or negative ΔH^\ddagger values for $k_{\text{on,high}}$ clearly reflect a preequilibrium step or steps (see above discussion, and Scheme 3). Further comparisons of ΔH^\ddagger with those obtained for other discrete binuclear copper(I) complexes are worthwhile (Table 2). The series of complexes [Cu₂(R-XYL-H)(O₂)]²⁺ (**6^R**) (Scheme 2) have the identical ligand set (i.e., the PY2 tridentate) linked instead by a xylyl group. We originally measured the kinetics and thermodynamics of the oxygenation of parent compound [Cu₂(H-XYL-H)]²⁺ (**5^H**)⁶⁰ and other analogues [Cu₂(R-XYL-H)]²⁺ (**5^H**) (R = *t*Bu, NO₂, F) in dichloromethane,^{10,33} and then more recently⁵⁶ **5^H** was restudied in acetone as solvent. As seen in Table 2, the ΔH^\ddagger values for all of these cases are similarly low.

Tolman, Zuberbühler, and co-workers^{42,61} have also studied the kinetics of formation of dioxygen complexes with binuclear

compounds containing substituted triazacyclononane (tacn) tridentate ligands, such as *i*-Pr₄dtne {1,2-bis(4,7-diisopropyl-1,4,7-triaza-1-cyclononyl)ethane} and *m*-XYL^{iPr4} { α,α' -bis(4,7-diisopropyl-1,4,7-triazacyclononan-1-yl)-*m*-xylene}. As seen in Table 2, these dicopper(I) oxygenation reactions exhibit ΔH^\ddagger values of ~39 kJ mol⁻¹. These considerably higher activation enthalpies, which compare to formation of Cu–O₂ 1:1 (i.e., cupric–superoxo) adducts in reactions of well-studied mononuclear copper(I) compounds with tmpa ($\Delta H^\ddagger = 32$ kJ mol⁻¹) and bqpa {(bis-2-quinolyl)(2-pyridyl)methylamine} ($\Delta H^\ddagger = 30$ kJ mol⁻¹),^{10,37} are thus concluded to correspond to rate-limiting formation of superoxo intermediates (i.e., Cu^I•••Cu^{II}–O₂⁻) which are not spectroscopically observable in these tacn derivative cases. It should be noted that the final (low-temperature) product of oxygenation for the *i*-Pr₄dtne complex is a bis- μ -oxo–dicopper(III) complex,⁶¹ while the *m*-XYL^{iPr4} dicopper(I) compound gives mixtures of μ - η^2 : η^2 -peroxo–dicopper(II) and bis- μ -oxo–dicopper(III) species.⁶² In comparing thermodynamic parameters for formation of dioxygen adducts within the series [Cu₂(Nn)(O₂)]²⁺ (**2^{Nn}**), we see that ΔH° values are essentially identical (-81 to -84 kJ mol⁻¹). Interestingly, the overall reaction enthalpy ΔH° values for the xylyl systems, [Cu₂(H-XYL-H)(O₂)]²⁺ (**6^H**), are considerably less negative (-42 in acetone to -62 kJ mol⁻¹ in CH₂Cl₂), perhaps reflecting steric hindrance or strain in Cu₂–O₂ bonding where the bulky and less flexible xylyl group connects PY2 tridentate moieties, compared to the situation for [Cu₂(Nn)(O₂)]²⁺ (**2^{Nn}**), with more flexible -(CH₂)_{*n*}- (*n* = 3–5) linkers. In fact, the systematic variation in corresponding ΔS° values results in the finding that the equilibrium constant for formation of **2^{Nn}** (K_1) increases with *n* value, at all temperatures (Table 1). For example, K_1 increases from 1.5 × 10⁴ to 3.5 × 10⁶ M⁻¹ going from the N3 to N5 complex (at 223 K), while K_1 (223 K) = 1.9 × 10⁴ M⁻¹ for [Cu₂(H-XYL-H)(O₂)]²⁺ (**6^H**).¹⁰ These findings are in accord with the view³⁴ that within the Nn series, the N5 complex forms a very favorable Cu₂–O₂ structure, which is relatively unstrained and most like the MePY2 complex [(MePY2)Cu]₂(O₂)]²⁺ (**4**) (which must be unstrained, being formed from mononuclear precursors; see also discussion above), where optimization of the Cu–O bonding occurs, and where a lowered $\nu(\text{O}–\text{O})$ value is observed.³⁴

Some other comparisons are worth mentioning. Strong dioxygen binding occurs in [(tmpa)Cu]₂(O₂)]²⁺ (see Introduction) with thermodynamic parameters (EtCN solvent, $\Delta H^\circ = -81$ kJ mol⁻¹, $\Delta S^\circ = -220$ J K⁻¹ mol⁻¹)¹⁰ which in fact compare closely to those of the present Nn complexes [Cu₂(Nn)(O₂)]²⁺ (**2^{Nn}**). A complex which possesses a binucleating analogue of tmpa (with -CH₂OCH₂-linked pyridyl groups, one from each tmpa moiety) is so stable in acetone that thermodynamic parameters could not be obtained (i.e., since its formation was essentially complete at all temperatures).³⁸ A corresponding ligand (**D¹**) with -CH₂CH₂- linker leads to a strained much less stable dioxygen adduct, [(**D¹**)Cu₂(O₂)]²⁺, with $\Delta H^\circ = -35$

(60) Cruse, R. W.; Kaderli, S.; Karlin, K. D.; Zuberbühler, A. D. *J. Am. Chem. Soc.* **1988**, *110*, 6882–6883.

(61) Mahapatra, S.; Young, Jr., V. G.; Kaderli, S.; Zuberbühler, A. D. *Angew. Chem., Int. Ed. Engl.* **1997**, *36*, 130–133.

kJ mol^{-1} , $\Delta S^\circ = -89 \text{ J K}^{-1} \text{ mol}^{-1}$.^{10,65} For a few other cases, limited kinetic or thermodynamic (but not both) data have been obtained and reported.^{11,66,67}

Oxygenation Behavior of Mononuclear Analogue [(MePY2)Cu(MeCN)]⁺ (3). As discussed in the Introduction, the spectroscopic properties of $[\{(\text{MePY2})\text{Cu}\}_2(\text{O}_2)]^{2+}$ (**4**), the low-temperature oxygenation product of **3**, have been described and compared with those of $[\text{Cu}_2(\text{Nn})(\text{O}_2)]^{2+}$ (**2^{Nn}**). We did previously report results of a kinetic study of the O_2 reaction with $[(\text{MePY2})\text{Cu}(\text{MeCN})](\text{BARF})$ (**3-(BARF)**) in acetone.²⁹ Oxygenation of **3-(BARF)** occurs in a second-order process (pseudo-first order in $[\text{O}_2]$), no intermediate is observed, and $\Delta H^\ddagger = -0.7 \pm 1 \text{ kJ M}^{-1}$, $\Delta S^\ddagger = -164 \pm 4 \text{ J K}^{-1} \text{ M}^{-1}$, $\Delta H^\circ = -89 \pm 3 \text{ kJ mol}^{-1}$, and $\Delta S^\circ = -240 \pm 9 \text{ J K}^{-1} \text{ M}^{-1}$. Here, we wished to examine the kinetics of oxygenation of $[(\text{MePY2})\text{Cu}(\text{MeCN})](\text{ClO}_4)$ (**3-ClO₄**) in dichloromethane, to directly compare to the results for $[\text{Cu}_2(\text{Nn})(\text{O}_2)]^{2+}$ (**2^{Nn}**), with the same solvent and same counteranion.

One obvious expectation was that the rates of oxygenation of the binuclear dicopper(I) complexes $[\text{Cu}_2(\text{Nn})(\text{MeCN})_2]^{2+}$ (**1^{Nn}**) and formation of intramolecular μ -peroxo complexes $[\text{Cu}_2(\text{Nn})(\text{O}_2)]^{2+}$ (**2^{Nn}**) would be faster than oxygenation of a corresponding mononuclear species, since an *intermolecular* reaction should yield a second-order kinetic process. Figure 4a gives a kinetic trace for the reaction of $[(\text{MePY2})\text{Cu}(\text{MeCN})]^+$ (**3**) with O_2 at 243 K. A significant induction period is observed, this pertaining to buildup of the 360 nm absorption of **4**. By contrast, the d-d band ($\sim 600 \text{ nm}$) starts forming immediately. Thus, oxidation of copper(I) is occurring, but generation of the μ -peroxo complex $[\{(\text{MePY2})\text{Cu}\}_2(\text{O}_2)]^{2+}$ (**4**) requires more reaction steps.⁶⁸ Once formation of **4** begins (360 nm band), maximum formation requires more than 30 s. By comparison, the oxygenation of $[\text{Cu}_2(\text{N4})(\text{MeCN})_2]^{2+}$ (**1^{N4}**) is complete in less than 5 s at 243 K (Figure 2). The rates of oxygenation of binuclear xylol complexes $[\text{Cu}_2(\text{R-XYL-H})]^{2+}$ (**5^R**) to form O_2 -adducts $[\text{Cu}_2(\text{R-XYL-H})(\text{O}_2)]^{2+}$ (**6^R**) are faster than $[(\text{MePY2})\text{Cu}(\text{MeCN})]^+$ (**3**) but slower than $[\text{Cu}_2(\text{Nn})(\text{MeCN})]^{2+}$ (**1^{Nn}**).

Also, the presence of acetonitrile has been found to significantly influence the kinetics of the oxygenation reactions for $[(\text{MePY2})\text{Cu}(\text{MeCN})]^+$ (**3**). Figure 4a–d shows the effect of the addition of 0, 1, 2 and 4 equivalents of acetonitrile. The oxygenation rates at 243 K (i.e., as judged by the time for maximum formation (360 nm) of the μ -peroxo product) decreased considerably with addition of acetonitrile. Added MeCN also seems to (i) inhibit full formation of $[\{(\text{MePY2})\text{Cu}\}_2(\text{O}_2)]^{2+}$ (**4**) (lower 360 nm absorption obtained) and (ii) increase the length of the induction period. These observations are consistent with the notion that MeCN, as a strong Cu(I) ligand,⁶⁹ influences the copper(I) complex preequilibrium and the dioxygen binding process.

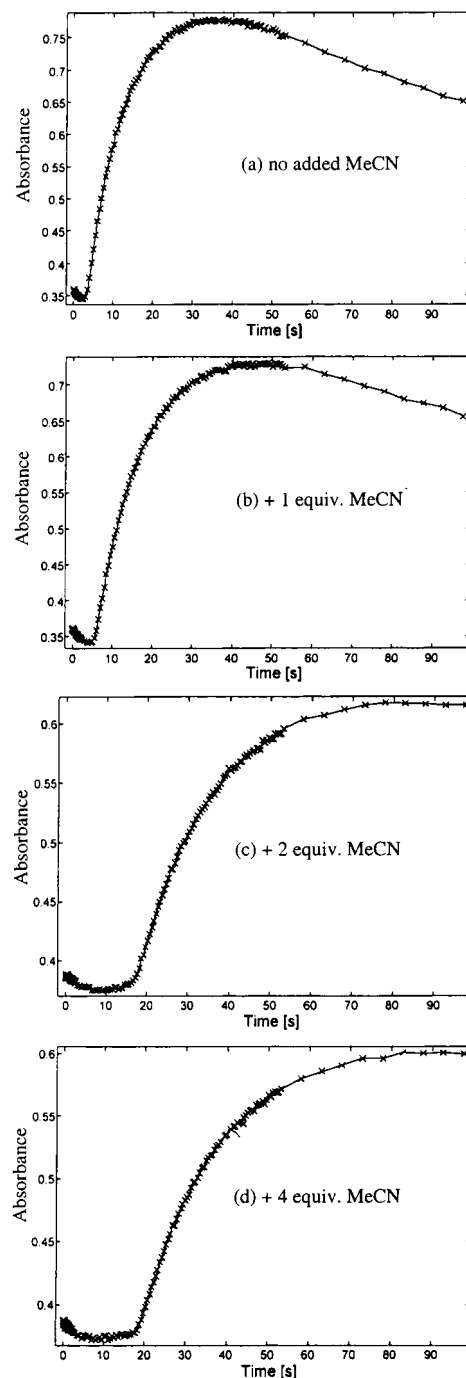


Figure 4. Effect of acetonitrile on the oxygenation of $[(\text{MePY2})\text{Cu}(\text{MeCN})]^+$ (**3**) to form $[\{(\text{MePY2})\text{Cu}\}_2(\text{O}_2)]^{2+}$ (**4**). Absorbance vs time at 360 nm: (a) no added MeCN yields shortest induction period and fastest full formation of **4**; (b) 1 equiv of added MeCN shows slightly longer induction period and slower rate of formation of **4**; (c) 2 equiv of added MeCN significantly increases the induction period and slows the rate of oxygenation (noticeable suppression of the formation of **4** (decreased absorbance) is also shown); (d) 4 equiv of added MeCN gives a similar result.

$[\text{Cu}_2(\text{O}_2)]^{2+}$ (**4**) (lower 360 nm absorption obtained) and (ii) increase the length of the induction period. These observations are consistent with the notion that MeCN, as a strong Cu(I) ligand,⁶⁹ influences the copper(I) complex preequilibrium and the dioxygen binding process.

Oligomerization of $[(\text{MePY2})\text{Cu}(\text{MeCN})]^+$ (**3**) in dichloromethane, especially at lower temperatures, also is likely. For

(62) In the well-studied reaction of a copper(I) complex with 1,4,7-triisopropyl-1,4,7-triazacyclononane (see refs 62 and 63), a solvent dependent formation of μ - η^2 : η^2 -peroxo-dicopper(II) and bis- μ -oxo-dicopper(III) species occurs, and $\Delta H^\ddagger = 37 \text{ kJ mol}^{-1}$ (in acetone, where a mixture forms), comparing closely to the binuclear cases mentioned here.

(63) Halfen, J. A.; Mahapatra, S.; Wilkinson, E. C.; Kaderli, S.; Young, V. G., Jr.; Que, L., Jr.; Zuberbühler, A. D.; Tolman, W. B. *Science* **1996**, *271*, 1397–1400.

(64) Cahoy, J.; Holland, P. L.; Tolman, W. B. *Inorg. Chem.* **1999**, *38*, 2161–2168.

(65) Lee, D.-H.; Wei, N.; Murthy, N. N.; Tyeklár, Z.; Karlin, K. D.; Kaderli, S.; Jung, B.; Zuberbühler, A. D. *J. Am. Chem. Soc.* **1995**, *117*, 12498–12513.

(66) Itoh, S.; Taki, M.; Nakao, H.; Holland, P. L.; Tolman, W. B.; Que, L., Jr.; Fukuzumi, S. *Angew. Chem., Int. Ed.* **2000**, *39*, 398–400.

(67) Santagostini, L.; Gullotti, M.; Monzani, E.; Casella, L.; Dillinger, R.; Tuczek, F. *Chem. Eur. J.* **2000**, *6*, 519–522.

(68) To speculate, initial outer-sphere oxidation of $[(\text{MePY2})\text{Cu}(\text{MeCN})]^+$ (**3**) by O_2 might explain the observed d-d band formation, prior to (i.e., induction period) O_2 -adduct (**4**) formation. Perhaps this occurs because the structure of a dimerized complex **3** (discussed below) disfavors O_2 -adduct formation, and its breakup is required to lead to **4**.

(69) Hathaway, B. J. In *Comprehensive Coordination Chemistry*; Wilkinson, G., Ed.; Pergamon: New York, 1987; Vol. 5; pp 533–774.

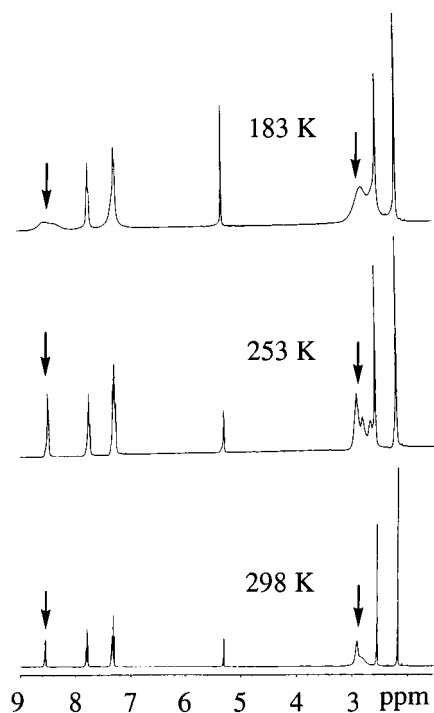


Figure 5. Variable-temperature ^1H NMR spectra for $[(\text{MePY}2)\text{Cu}(\text{MeCN})]^+$ (**3**), demonstrating its fluxional nature by observation of changes (see arrows) in pyridyl (downfield) and methylene (upfield) resonances of the tridentate MePY2 ligand. This behavior is consistent with the presence of mixtures of monomeric and dimeric forms of **3**. See text for further discussion.

the oxygenation of **3**, we found that the $t_{1/2}$ for formation of $[(\text{MePY}2)\text{Cu}]_2(\text{O}_2)^{2+}$ (**4**) to be constant with increasing concentration of the complex, not consistent with second-order behavior. This phenomenon may be rationalized by dimerization of **3** at low temperatures, as suggested to also occur for binuclear Nn analogues $[\text{Cu}_2(\text{Nn})(\text{MeCN})_2]^{2+}$ (**1^{Nn}**). Support of this hypothesis comes from examination of the variable-temperature ^1H NMR spectra of **3** in dichloromethane. By adding MeCN (~ 10 equiv) to ensure breakup of any dimers and to shift the equilibrium to favor the species $[(\text{MePY}2)\text{Cu}(\text{MeCN})]^+$ (**3**), a sharp and fully assignable spectrum is obtained over the temperature range of 183–318 K, consistent with this mononuclear formulation. By comparison, the ^1H NMR spectrum of **3** at 298 K (without added MeCN) already shows broadened methylene signals (2.7 to 3.1 ppm), which sharpen and again broaden on going to lower temperatures (to 183 K) (Figure 5). Thus, there is clear indication of dynamic behavior. In addition, the 6-pyridyl proton signal at 8.55 ppm (doublet) at 298 K starts to broaden at 203 K and becomes a very broad unsymmetrical multiplet at 183 K (Figure 5). The complicated spectral behavior reflects structural changes, but detailed interpretation is not possible, especially since limiting behavior is not achieved even over the temperature range of 183–298 K. Clearly, further work is needed to clarify the true nature of the copper(I) species present in solution which reacts with dioxygen.

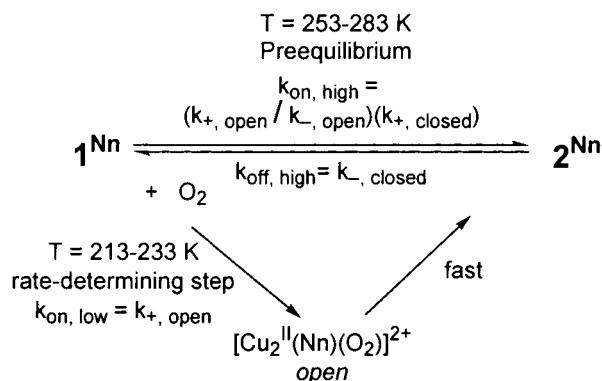
Summary

The complexes $[\text{Cu}_2(\text{Nn})(\text{MeCN})_2]^{2+}$ (**1^{Nn}**) and close mononuclear analogue $[(\text{MePY}2)\text{Cu}(\text{MeCN})]^+$ (**3**), which form μ - η^2 : η^2 -peroxodicopper(II) complexes $[\text{Cu}_2(\text{Nn})(\text{O}_2)]^{2+}$ (**2^{Nn}**) and $[(\text{MePY}2)\text{Cu}]_2(\text{O}_2)^{2+}$ (**4**), respectively, comprise a series of compounds of interest in terms of their reversible dioxygen binding behavior (for **1^{Nn}**),^{17,35,36} their systematic variation in spectroscopic and structural features,²⁸ solution versus solid-

state structure,³² and reactivity toward exogenous substrates.²⁹ The study here was undertaken to add to our fundamental base of knowledge of kinetic–thermodynamic behavior, which is still quite limited for copper–dioxygen reactivity in well-characterized systems. The main conclusions or findings presented are as follows.

(1) Reactions of $[\text{Cu}_2(\text{Nn})(\text{MeCN})_2]^{2+}$ (**1^{Nn}**) with O_2 in dichloromethane occur with rapid formation of intramolecular μ -peroxo species.

(2) The overall kinetic mechanism involves sequential reversible reactions, the first involving O_2 -adduct formation giving a nondetectable “open” intermediate followed by closure to give the μ -peroxo final product, $[\text{Cu}_2(\text{Nn})(\text{O}_2)]^{2+}$ (**2^{Nn}**). Data analysis yields a break in the Eyring plots between a higher and lower temperatures domain. At higher temperatures (253–283 K), the data fit a simple reversible binding equilibrium process, while in the range of 213–233 K, the first step is rate-limiting.



(3) For either temperature regime, the ΔH^\ddagger for formation of $[\text{Cu}_2(\text{Nn})(\text{O}_2)]^{2+}$ (**2^{Nn}**) are low, in some cases negative, reflecting the occurrence of preequilibria, most assuredly at least involving superoxo–copper(II) species $\text{Cu}^{\text{II}}\cdots\text{Cu}^{\text{II}}\text{--O}_2^-$. However, no intermediates could be spectroscopically observed.

(4) At still lower temperatures, below 213 K, a complicated behavior for oxygenation of $[\text{Cu}_2(\text{Nn})(\text{MeCN})_2]^{2+}$ (**1^{Nn}**) occurs. Oligomerization of **1^{Nn}** is suggested to account for the unexpected finding that the half-life for formation of $[\text{Cu}_2(\text{Nn})(\text{O}_2)]^{2+}$ (**2^{Nn}**) increases with, rather than being independent of the concentration of **1^{Nn}**. There exists strong literature precedent for oligomerization of these types of compounds.

(5) Overall, there are relatively small differences in the kinetic and thermodynamic parameters observed for formation of $[\text{Cu}_2(\text{Nn})(\text{O}_2)]^{2+}$ (**2^{Nn}**). Strong complexes form, with ΔH° in the narrow range between -81 and -84 kJ mol^{-1} . As is usual,^{4,10} compensating large negative entropies of formation are observed (Table 1). Yet, we note that the equilibrium constant for formation of **2^{Nn}** (K_1) increases on going from the N3 to N4 to N5 complex. This observation seems in accord with differences in structure and spectroscopy (i.e., $\nu(\text{O}=\text{O})$) among the Nn complexes $[\text{Cu}_2(\text{Nn})(\text{O}_2)]^{2+}$ (**2^{Nn}**).²⁸

(6) The low ΔH^\ddagger values (i.e., reflecting preequilibria) for formation of $[\text{Cu}_2(\text{Nn})(\text{O}_2)]^{2+}$ (**2^{Nn}**) are similarly observed for the well-studied series of xylyl complexes $[\text{Cu}_2(\text{R-XYL-H})(\text{O}_2)]^{2+}$ (**6^R**). However, the present complexes **2^{Nn}** exhibit significantly more favorable ΔH° values (-81 to -84 kJ mol^{-1}) than for **6^R** (-52 to -74 kJ mol^{-1}), perhaps reflecting the presence of a stiffer and bulkier xylyl linker in $[\text{Cu}_2(\text{R-XYL-H})(\text{O}_2)]^{2+}$ (**6^R**) compared to the methylene chain connector in $[\text{Cu}_2(\text{Nn})(\text{O}_2)]^{2+}$ (**2^{Nn}**).^{4,10}

(7) The O_2 -reaction chemistry with $[(\text{MePY}2)\text{Cu}(\text{MeCN})]^+$ (**3**) in dichloromethane is complicated, including the presence

of induction periods, and quantitative kinetic–thermodynamic parameters could not be obtained. Nevertheless, qualitative comparisons clearly show that the intermolecular second-order reaction of 2 equiv of **3** with O₂ to form [$\{(\text{MePY}2)\text{Cu}\}_2(\text{O}_2)\]^{2+}$ (**4**) is much slower than that for the intramolecular reactions of $[\text{Cu}_2(\text{Nn})(\text{MeCN})_2]^{2+}$ (**1^{Nn}**) which give $[\text{Cu}_2(\text{Nn})(\text{O}_2)]^{2+}$ (**2^{Nn}**).

(8) The $t_{1/2}$ for formation of [$\{(\text{MePY}2)\text{Cu}\}_2(\text{O}_2)\]^{2+}$ (**4**) is found to be constant with increasing concentration of the complex, while a decrease is to be expected. Variable-temperature ¹H NMR data reveal solution dynamic behavior. The unusual concentration dependence of the oxygenation of $[(\text{MePY}2)\text{Cu}(\text{MeCN})]^+$ (**3**) is thus explained by dimerization of the latter in solution, which is as mentioned a common phenomenon for copper(I) chelates of this type.

(9) Acetonitrile is found to significantly influence the kinetics of the oxygenation reactions for $[(\text{MePY}2)\text{Cu}(\text{MeCN})]^+$ (**3**). The oxygenation rates for the formation of the μ -peroxo product slowed considerably with addition of small amounts of acetonitrile. Added MeCN also inhibits full formation of [$\{(\text{MePY}2)$ -

$\text{Cu}\}_2(\text{O}_2)\]^{2+}$ (**4**) and increases the length of the induction period. Pertaining to the last point, the presence of MeCN, even 1 equiv per copper(I) ion, appears to block observance of an additional dioxygen adduct intermediate (at least for the oxygenation of $[\text{Cu}_2(\text{N}4)(\text{MeCN})_2]^{2+}$ (**1^{N4}**) (vide supra); further studies of complexes with absolutely no MeCN present are planned. Our future kinetic–thermodynamic studies of copper–dioxygen chemistry will also address electronic and/or solvent effects in reversible O₂-binding chemistry, and O₂-reactions which are followed by substrate oxidation.

Acknowledgment. We are grateful to the National Institutes of Health (K.D.K.; GM28962) and the Swiss National Science Foundation (A.D.Z.) for support of this research.

Supporting Information Available: Eyring plots for $k_{\text{on,low}}$, $k_{\text{on,high}}$, and $k_{\text{off,high}}$ for the N3 and N5 complexes. This material is available free of charge via the Internet at <http://pubs.acs.org>.

IC0007916